

ENERGY SPECTRA OF PHOTOPROTONS FROM ALUMINIUM, SULPHUR, AND SILICON

By H. LICHTBLAU*† and B. M. SPICER*

[Manuscript received January 17, 1966]

Summary

Energy distributions of photoprotons emitted at 90° to the bombarding X-ray beam of the Melbourne 35 MeV betatron from thin targets of natural aluminium, sulphur, and silicon, measured with a scintillation spectrometer incorporating pulse-shape discrimination (PSD), are presented. The ^{27}Al proton spectrum, whose shape is found to be inconsistent with predominant evaporation of particles from a compound nucleus, exhibits a "hump" at 8.6 MeV, which is attributed to transitions between known levels in target and residual nuclei.

Comparisons of the photoproton spectra from silicon and sulphur with simple particle-hole model calculations indicate that simultaneous agreement of the theory with observed locations of giant resonances and decay modes is not obtainable.

INTRODUCTION

Before the development of pulse-shape discrimination (PSD) techniques (see Owen 1962), the study of (γ, p) reactions with bremsstrahlung X-rays was largely carried out with the aid of nuclear emulsions, because the abundant background rendered electronic pulse detection methods unsuitable. Besides being laborious, nuclear emulsion work rarely provides satisfactory statistical accuracy.

The scintillation spectrometer used in the present investigations achieves a high degree of insensitivity to background by means of a PSD system (Varga 1961), thus making it possible to measure the energies of photoprotons emitted from bremsstrahlung-irradiated targets down to energies of about 2 MeV and, hence, to perform systematic studies of (γ, p) reactions.

EXPERIMENTAL ARRANGEMENT

A schematic diagram of the target chamber together with lead shielding and scintillator-photomultiplier assembly, designed to detect particles ejected at right angles to the X-ray beam, is shown in Figure 1. The bombarding beam, which is collimated to have a diameter of $\frac{11}{16}$ in. in the middle of the target chamber, enters and leaves the chamber through 10^{-3} in. (3.5 mg/cm^2) Mylar windows. Solid targets are mounted centrally in the chamber, with their plane parallel to the flat surface of the $\frac{1}{8}$ in. thick CsI(Tl) scintillator, which has an effective diameter of $\frac{7}{8}$ in. and is mounted on a $\frac{1}{2}$ in. high conical glass light pipe.

* School of Physics, University of Melbourne.

† Present address: Institut für Technische Kernphysik, Technische Hochschule, Darmstadt, West Germany.

For studying photoparticles from gas targets, the chamber can be filled to the desired pressure with the gas in question. In this case, a 0.5×10^{-3} in. (1.75 mg/cm^2) Mylar foil separates the target chamber from the evacuated section containing the CsI(Tl) crystal.

Under normal running conditions, the full width at half maximum of the 8.8 MeV alpha line of $\text{ThC} + \text{C}'$ is approximately 350 keV. Radiation dose was measured with a thick-walled NBS ionization chamber (Pruitt and Domen 1962).

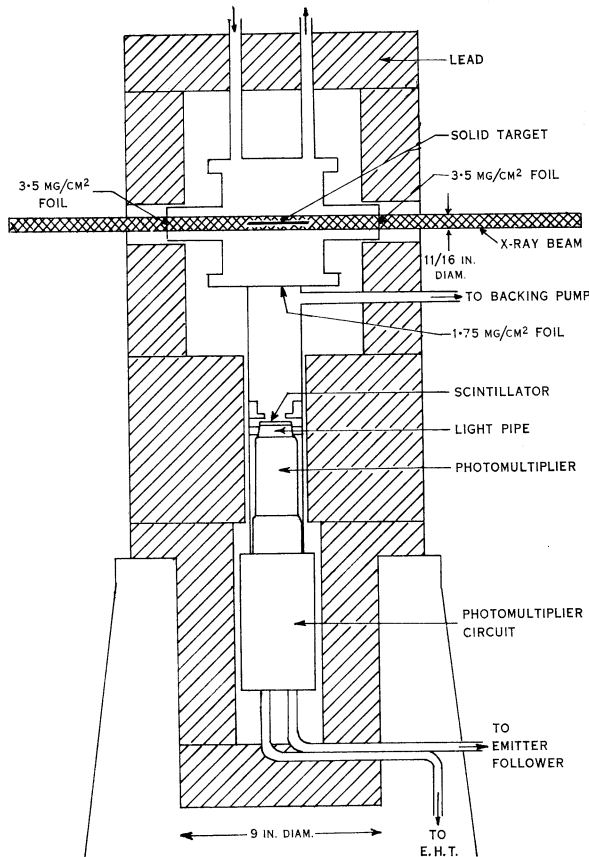


Fig. 1.—Diagram of vertical section through spectrometer and lead shielding assembly. Scintillator and photomultiplier are situated inside a lead cylinder of wall thickness 5.5 in.

PULSE-SHAPE DISCRIMINATION SYSTEM

A block diagram of the electronics is given in Figure 2. Pulses due to the motion of charged particles in the CsI(Tl) crystal formed at the anode of the phototube (EMI type 9536A) are clipped by a shorted RG65/U delay cable after rising to a height that corresponds to the total energy of the exciting particle.

Subsequently, the pulses are fed into two separate channels. One channel leads via a further clipping stage to the signal input of a 512 channel RCL pulse-height analyser. Along the other channel, the pulses are delay line-shaped by another RG65/U cable, terminated so that an opposite polarity "spike" signal is formed whenever the pulse has the fast rise characteristic of heavy particle excitations. The spikes trigger gate pulses, admitting the total-light output signals into the analyser. Background-excited pulses, having longer rise times corresponding to the slower decay of electron-generated scintillations, do not acquire spikes and are, therefore, not registered.

The various clipping and shaping stages are separated by emitter followers. Prompt coincidence gate pulses synchronize the operation of the analyser with the X-ray bursts of the betatron.

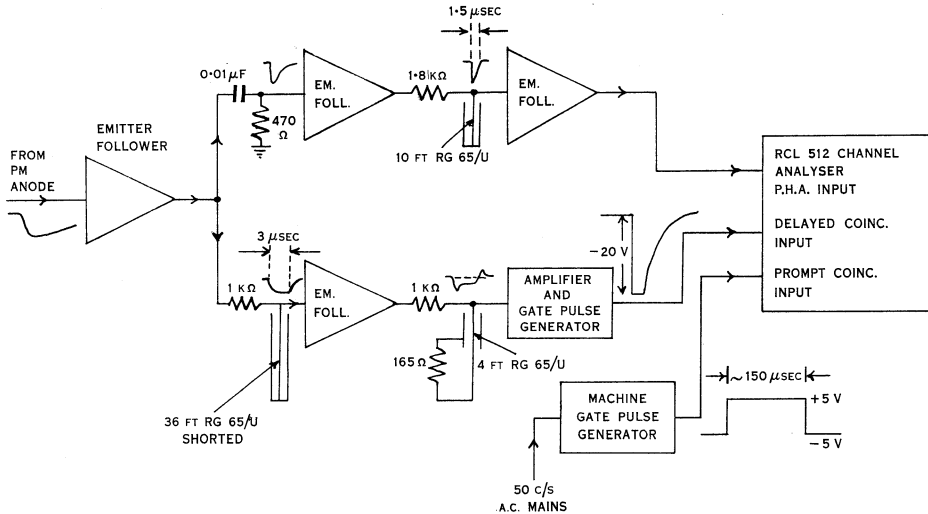


Fig. 2.—Block diagram of PSD electronics.

CALIBRATION

As a supply of monoenergetic protons was not available, the spectrometer was calibrated by reference to the known energies (Dodge and Barber 1962; Firk and Lokan 1962; Tanner, Thomas, and Earle 1964; Yergin *et al.* 1964) of three prominent proton groups formed in the $^{16}\text{O}(\gamma, p)^{15}\text{N}$ reaction. Energy losses suffered by the protons in the gas and in traversing the Mylar foil were estimated from the data of Whaling (1958).

Figures 3(a) and 3(b) are pulse-height spectra of charged photoparticles emitted in the $^{16}\text{O}(\gamma, p)^{15}\text{N}$ reaction. The end-point energy of the bombarding radiation was 32 MeV. Comparison of these spectra with each other demonstrates the advantage of PSD. In the spectrum of Figure 3(a), which was taken with the PSD part of the electronics turned off, photoparticles below channel 60 (corresponding to ~ 7 MeV protons) are masked by background counts. The spectrum of Figure 3(b) was recorded under the same conditions as for the spectrum of Figure 3(a), except

that PSD was operating normally. Here, freedom from background interference persists right down to the lower level cutoff in channel 15.

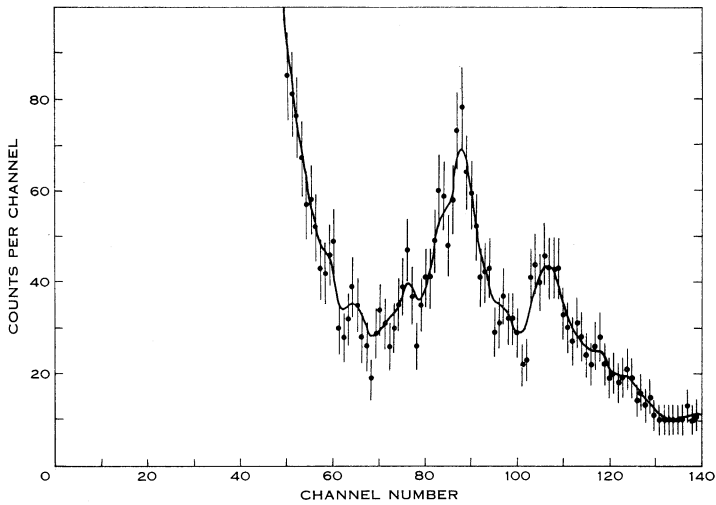


Fig. 3(a).— $^{16}\text{O}(\gamma, p)^{15}\text{N}$ 90° proton spectrum without PSD. This spectrum gives information relating to protons whose energy of emission exceeds 6.7 MeV.

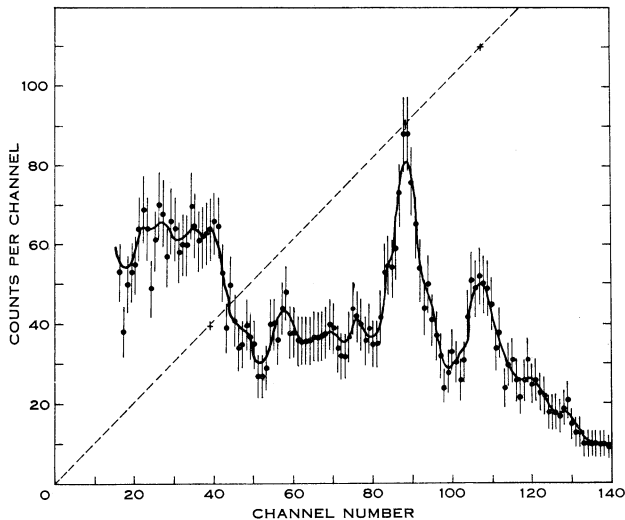


Fig. 3(b).— $^{16}\text{O}(\gamma, p)^{15}\text{N}$ 90° proton spectrum with PSD. This spectrum was recorded under the same experimental conditions as for the spectrum of Figure 3(a), except that the PSD was operating. The dashed line, which adequately fits the calibration points, corresponds to 0.102 MeV per channel.

The curves fitted to the experimental points of Figure 3, as well as those in subsequent figures, were obtained by the smoothing procedure of Ferreira and

Valoshek (1955). Figure 3(b) also contains the three calibration points of the laboratory proton-energy versus channel-number curve, corresponding to the peaks of the proton groups formed in transitions to the ground state of ^{15}N from ^{16}O resonances (Dodge and Barber 1962; Firk and Lokan 1962; Tanner, Thomas, and Earle 1964; Yergin *et al.* 1964) at 17.3, 22.3, and 24.3 MeV, indicated by their error bars. These points agree, within a small fraction of the experimental errors, with the expected linear relationship (Fig. 3(b)) between proton energy and pulse height.

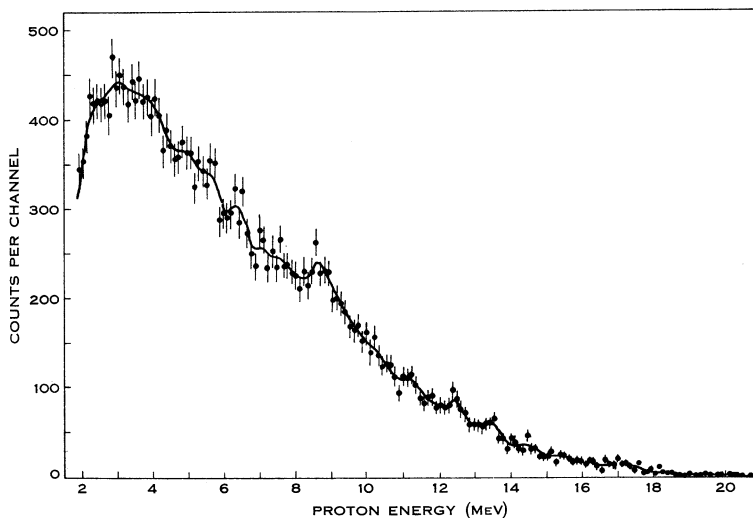


Fig. 4.—Energy spectrum of photoprotons from aluminium, with bremsstrahlung end-point energy 32 MeV.

ALUMINIUM

Figure 4 shows the measured energy distribution of the 90° photoprotons from a 6.7 mg/cm^2 ^{27}Al target irradiated with 32 MeV bremsstrahlung X-rays. The most conspicuous structural feature of the spectrum is the “hump” at 8.6 MeV. At this proton energy, there is also a change in the overall slope of the spectral curve. While nuclear emulsion work (Diven and Almy 1950; Dawson 1956; Shoda *et al.* 1961) failed to reveal this feature, the irregularity was observed in the electrodisintegration experiments of Dodge and Barber (1962).

The isotropic angular distribution of the photoprotons and the lack of structure in the energy spectrum are consistent with the statistical model (Weisskopf and Ewing 1940), which assumes that the protons are emitted from a compound nucleus by an evaporation mechanism. According to this model, the energy spectrum of the evaporated nucleons is given by the Maxwellian distribution law

$$N(E) dE = \text{const. } E \exp(-E/\theta) dE, \quad (1)$$

where E is the kinetic energy of the emitted particle, θ is the effectively constant nuclear temperature of the target nucleus, and the quantity $\exp(-E/\theta)$ is proportional to the level density $\omega(E_r)$ in the residual nucleus at excitation energy

$E_r = E_m - E$, E_m being the highest energy attainable by the ejected particle at a given excitation of the target nucleus.

The observable spectrum $n(E)$ is related to (1) by

$$n(E) = TN(E), \quad (2)$$

where T is the appropriate coefficient for the transmission of the particle in question through the combined Coulomb and centrifugal barriers. Assuming θ to be constant,

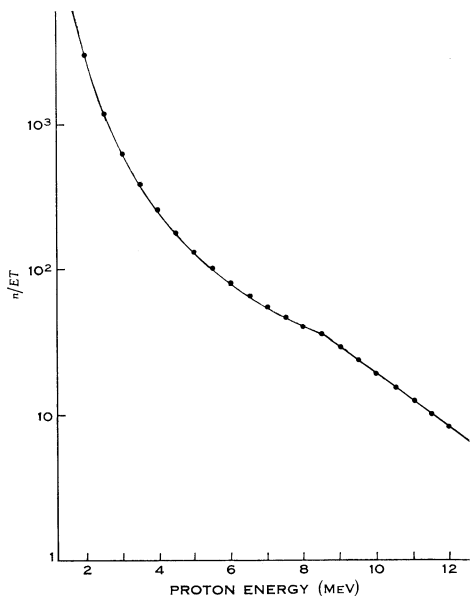


Fig. 5.—Log-linear plot of n/ET versus proton energy E , constructed from the data of Figure 4.

the bremsstrahlung spectrum will not influence the shape of the photoparticle spectrum.

From (1) and (2), we have

$$\log\{n(E)/ET\} = \text{const.} (-E/\theta). \quad (3)$$

To test the spectrum of Figure 4 for compatibility with (3), all doubtful local fluctuations were smoothed out, and the ordinates thus obtained were treated as a measure of $n(E)$. The transmission coefficients for the penetration of protons into ^{26}Mg were extracted from the tables of Feshbach, Shapiro, and Weisskopf (1953), assuming effectively pure p -wave penetration to give an adequate description.

From the log-linear plot of n/ET versus E thus derived, shown in Figure 5, the linear relation demanded by (3) is seen to be obeyed only for protons of energies above 8.6 MeV. This suggests that few, if any, of the photonucleons are evaporated from a compound nucleus, because at any reasonable nuclear temperature the evaporation mechanism dominates at the lower energies, and the "break" is associated with the energy at which evaporation has sufficiently decreased for direct emission to become important.

Resonances of ^{27}Al have been measured by $^{27}\text{Al}(\gamma, n)$ yield curve studies (Thompson *et al.* 1965) and total nuclear absorption experiments (Dular *et al.* 1959; Ziegler 1960; Wyckoff *et al.* 1965), while information on low-lying levels in ^{26}Mg has been compiled by Endt and Van der Leun (1961). Of the known ^{27}Al excitations (Thompson *et al.* 1965), only those at 21.2 and 22.4 MeV are compatible with decays to established $^{26}\text{Mg}^*$ states by emission of ~ 8.6 MeV protons. The corresponding levels in ^{26}Mg are at 4.0 and 5.2 MeV respectively.

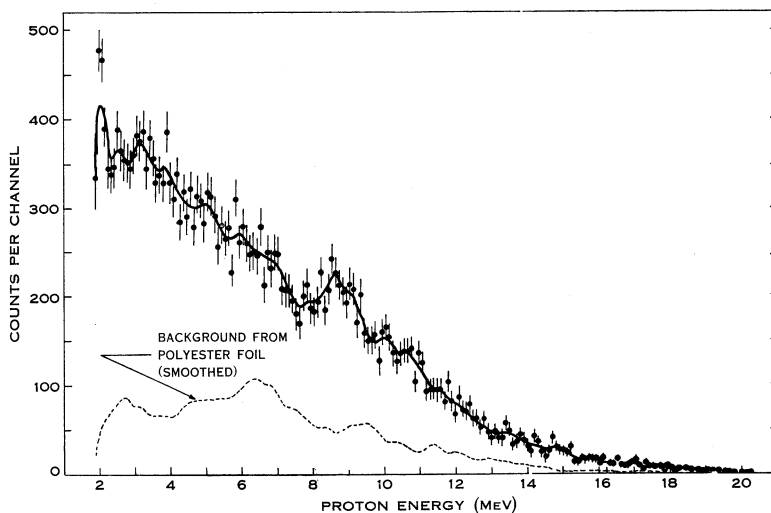


Fig. 6.—Energy spectrum of photoprotons from sulphur, with bremsstrahlung end-point energy 32 MeV.

According to a theoretical treatment (Baglin, Thompson, and Spicer 1961; Thompson *et al.* 1965) of the giant resonance of ^{27}Al , based on the Nilsson single-particle level scheme, the ^{27}Al excitation at the higher energy is a $1p_{1/2}^{-1}d_{3/2}$ configuration, which excludes this level from contributing to the observed hump, because the hole in the p -shell leaves ^{26}Mg in a too highly excited state to allow the emission of 8.6 MeV protons. Since no such restrictions apply to the other resonance in ^{27}Al , we suggest that the knee in the proton spectrum of Figure 5 at 8.6 MeV is formed by proton decay of the 21.2 MeV resonance of ^{27}Al to the 3.94 MeV state in ^{26}Mg .

SULPHUR

Figure 6 shows the laboratory energy spectrum of the photoprotons from sulphur emitted at 90° to the 32 MeV bremsstrahlung beam. The target was a 6.45 mg/cm² deposit of natural sulphur on a 0.88 mg/cm² Mylar foil prepared by the method of Nielsen and Weinstein (1953). The spectrum of the photoparticles emitted from the foil alone, which was determined by separate runs and subtracted from the total count spectrum, is indicated in the figure by the broken line.

Natural sulphur consists predominantly of ^{32}S . The giant resonance of this closed subshell nucleus has recently been treated theoretically by Spicer (1965),

who performed a Tamm–Dancoff approximation particle–hole model calculation of the energy eigenvalues, eigenvectors, and strengths of the electric dipole excitations. This calculation predicts that the bulk of the dipole strength is concentrated on a ~ 19 MeV state whose predominant configuration is $1d_{5/2}^{-1}1f_{7/2}$.

If Spicer's calculation gives an adequate description of the giant resonance of ^{32}S , the most prominent group in the spectrum of Figure 6 should be formed by the protons emitted in transitions from a ~ 19 MeV level of ^{32}S to a $\frac{5}{2}^+$ single-hole state in ^{31}P . Spicer assumes that the $\frac{5}{2}^+$ level in question is located 5 MeV above the ground state of ^{31}P . He supports this assignment by experimental data obtained in $^{32}\text{S}(p, 2p)^{31}\text{P}$ reaction studies (Pugh and Riley 1961; Gottschalk 1962).

TABLE 1

ENERGY EIGENVALUES, DIPOLE STRENGTHS, AND EIGENVECTORS FOR $1^-, T = 1$ STATES IN ^{32}S
Eigenvectors are not normalized

Energy (MeV)	Dipole Strength (%)	$2s_{1/2}^{-1}2p_{3/2}$	$1d_{5/2}^{-1}1f_{7/2}$	$1d_{5/2}^{-1}2p_{3/2}$	$2s_{1/2}^{-1}2p_{1/2}$	$1d_{5/2}^{-1}1f_{5/2}$	$1p_{1/2}^{-1}1d_{3/2}$	$1p_{5/2}^{-1}1d_{3/2}$
Unmodified (Spicer 1965)*								
11.89	5	1.000	-0.155	0.016	-0.188	0.020	-0.010	0.007
14.07	2	0.152	-0.234	0.066	1.000	-0.091	-0.024	-0.026
16.77	2	-0.061	-0.177	1.000	-0.105	-0.096	0.096	0.023
19.07	58	0.183	1.000	0.254	0.204	0.220	-0.248	0.009
22.26	1	-0.057	-0.263	0.064	0.028	1.000	-0.133	-0.115
28.29	24	0.053	0.199	-0.029	0.072	0.159	1.000	-0.255
38.02	8	0.004	0.010	-0.023	0.048	0.148	0.225	1.000
Modified								
11.81	2.5	1.000	-0.236	0.006	-0.153	0.017	-0.003	0.004
13.77	1	0.050	-0.437	0.391	1.000	-0.173	0.026	-0.019
14.54	3.5	-0.072	-0.018	1.000	-0.404	-0.039	0.073	0.029
17.05	63	0.288	1.000	0.215	0.378	0.206	-0.221	-0.001
19.98	3.5	-0.066	-0.241	0.059	0.048	1.000	-0.104	-0.103
28.18	25	0.051	0.161	-0.026	0.068	0.120	1.000	-0.244
37.98	1.5	0.003	0.009	-0.021	0.048	0.128	0.223	1.000

* An error in this paper has been corrected.

Cross-section measurements of the reactions $^{32}\text{S}(\gamma, p)$ (Ishkanov *et al.* 1964) and $^{32}\text{S}(\gamma, n)$ (Thompson, Taylor, and Webb 1965), as well as total nuclear absorption measurements (Dular *et al.* 1959; Wyckoff *et al.* 1965), indicate that the main giant resonance maximum of ^{32}S corresponds to excitation energies between 19 and 21 MeV, in reasonable agreement with the calculation (Spicer 1965). Protons emitted from resonances in this energy region in transitions to a 5 MeV state in ^{31}P would have energies between 5 and 7 MeV. The spectrum of Figure 6 shows, however, no evidence for a major proton group between these energies.

Evidence for a $\frac{5}{2}^+$ level in ^{31}S at 2.4 MeV was found by Kavaloski, Cassani, and Hintz (1963) in the course of investigations of the energies and angular distri-

butions of the deuterons from the $^{32}\text{S}(p, d)^{31}\text{S}$ pick-up reaction. The corresponding level in ^{31}P is situated at 2.2 MeV. If the ^{31}P nucleus is left in this state following the decay of $^{32}\text{S}^*$ from the giant resonance, the peak in the proton group would occur between 7.7 and 9 MeV.

Since the strongest peak in the spectrum of Figure 6 was found within this energy range, the particle-hole calculation of Spicer (1965) was revised accordingly. The results of Spicer's original calculation, together with those obtained after modifying the level scheme of unperturbed particle and hole states by raising the $1d_{5/2}$ state by 2.35 MeV, are given in Table 1.

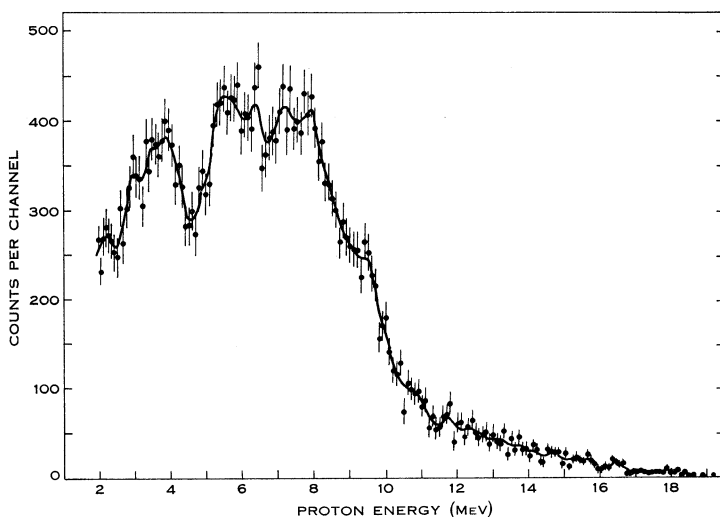


Fig. 7.—Energy spectrum of photoprotons from silicon, with bremsstrahlung end-point energy 32 MeV.

Comparison of the two sets of results demonstrates how critically the calculated distribution of dipole strengths depends on the choice of the unperturbed particle and hole states. Although the alteration consists only of a 2.35 MeV shift of a single level, the modified dipole strengths do not agree with observations.

One is thus faced with the dilemma of either adopting an unperturbed level scheme that leads to the right excitation energy of the giant resonance peak near 20 MeV, but forbids transitions which would account for the strong proton group between 8 and 9 MeV in the spectrum of Figure 6, or of assuming unperturbed states that agree with what appears to be the predominant mode of decay but are incapable of yielding the correct location of the giant resonance region.

SILICON

A 9.14 mg/cm² silicon target placed on a 0.88 mg/cm² Mylar foil was irradiated with 32 and 21.2 MeV bremsstrahlung X-rays. The loss-corrected (Whaling 1958) laboratory energy spectra of the photoprotons emitted at 90° to the incident beam

are shown in Figures 7 and 8. As in the case of sulphur, the contribution of the Mylar foil has been subtracted.

The peaks at 6.3, 7.2, 7.9, and 10 MeV can be identified with transitions to the ground state or to the first two excited states of ^{27}Al from $^{28}\text{Si}^*$ resonances found in other experiments (Caldwell *et al.* 1963; Koch 1964; Ullrich 1964; Cannington *et al.* 1965; Matsumoto *et al.* 1965). Three of these resonances are predicted by the particle-hole model calculations of Bolen and Eisenberg (1964), but the strong 18 MeV excitation, reflected by the proton groups at 6.3 and 5.5 MeV, is not accounted for by this model, which also indicates an unobserved spin-flip level near 26 MeV. Nevertheless, the Bolen-Eisenberg calculation is largely successful as far as the prediction of the major resonances in ^{28}Si is concerned.

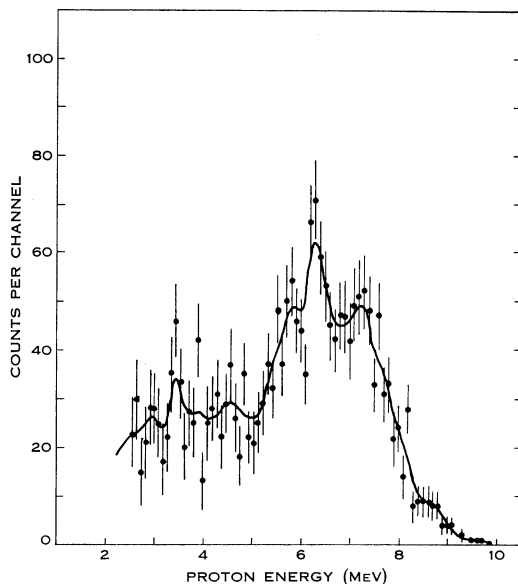


Fig. 8.—Energy spectrum of photoprotons from silicon, with bremsstrahlung end-point energy 21.2 MeV.

As in the case of ^{32}S , there is, however, strong evidence that the participating configurations are not restricted to those allowed by the unperturbed level scheme. Both the present experiments and other work (Ullrich 1964; Cannington *et al.* 1965; Matsumoto *et al.* 1965) show a considerable number of decays from ^{28}Si resonances to the 0.8 or 0.97 MeV levels of ^{27}Al , or both, which do not correspond to any of the unperturbed hole states assumed by Bolen and Eisenberg. It thus appears that the Tamm-Dancoff approximation, which limits the vector space to one that is entirely spanned by the few eigenstates of the unperturbed level schemes, is too drastic a simplification to yield a detailed description of the giant resonances of the closed subshell nuclei ^{32}S and ^{28}Si , where deformations are bound to remove degeneracies to a far greater extent than in doubly magic nuclei.

ACKNOWLEDGMENTS

This work was supported by a Research Grant from the U.S. Army Research Office.

The authors wish to thank Dr. J. M. Eisenberg for pointing out errors in the lower part of Table 1, which has been corrected in proof.

REFERENCES

- BAGLIN, J. E. E., THOMPSON, M. N., and SPICER, B. M. (1961).—*Nucl. Phys.* **22**: 216.
- BOLEN, L. N., and EISENBERG, J. M. (1964).—*Phys. Lett.* **9**: 52.
- CALDWELL, J. T., HARVEY, R. R., BRAMBLETT, R. L., and FULTZ, S. C. (1963).—*Phys. Lett.* **6**: 213.
- CANNINGTON, P. H., STEWART, R. J. J., HOGG, G. R., LOKAN, K. H., and SARGOOD, D. G. (1965).—*Nucl. Phys.* **72**: 23.
- DAWSON, W. K. (1956).—*Can. J. Phys.* **34**: 1480.
- DIVEN, B. C., and ALMY, G. M. (1950).—*Phys. Rev.* **80**: 407.
- DODGE, W. R., and BARBER, W. C. (1962).—*Phys. Rev.* **127**: 1746.
- DULAR, J., KERNEL, G., KREGAR, M., MIHAILOVIC, M. V., PREGL, G., ROSINA, M., and ZUPANCIC, C. (1959).—*Nucl. Phys.* **14**: 131.
- ENDT, P. M., and VAN DER LEUN, C. (1961).—*Nucl. Phys.* **34**: 1.
- FERREIRA, E. P., and VALOSHEK, P. Y. (1955).—Proc. First Int. Conf. Peaceful Uses Atom. Energy, Vol. 2. p. 124.
- FESHBACH, H., SHAPIRO, M. M., and WEISSKOPF, V. F. (1953).—"Tables of Penetrabilities for Charged Particle Reactions." U.S.A.E.C. Rep. No. NYO-3077. (Nuclear Development Associates, Inc.: White Plains, N.Y.)
- FIRK, F. W. K., and LOKAN, K. H. (1962).—*Phys. Rev. Lett.* **8**: 321.
- GOTTSCHALK, B. (1962).—Ph.D. Thesis, Harvard University.
- ISHKANOV, B. S., KAPITONOV, I. M., SCHEVCHENKO, V. G., and YUREV, B. A. (1964).—*Phys. Lett.* **9**: 162.
- KAVALOSKI, C. D., BASSANI, G., and HINTZ, N. M. (1963).—*Phys. Rev.* **132**: 813.
- KOCH, H. W. (1964).—*Nucl. Instrum. Meth.* **28**: 199.
- MATSUMOTO, S., YAMASHITA, H., KAMAE, T., and NOGAMI, Y. (1965).—*J. Phys. Soc. Japan* **20**: 1321.
- NIELSEN, E., and WEINSTEIN, A. (1953).—*Rev. Sci. Instrum.* **24**: 1146.
- OWEN, R. B. (1962).—*I.R.E. Trans. Nucl. Sci.* **9**: 285.
- PRUITT, J. S., and DOMEN, S. R. (1962).—*J. Res. Natn. Bur. Stand.* **66A**: 371.
- PUGH, H. G., and RILEY, K. F. (1961).—Proc. Rutherford Jubilee Int. Conf. p. 195. (Academic Press: New York.)
- SHODA, K., ISHIZUKA, T., SHIMIZU, K., and AKASHI, M. (1961).—*J. Phys. Soc. Japan* **17**: 1535.
- SPICER, B. M. (1965).—*Aust. J. Phys.* **18**: 1.
- TANNER, N. W., THOMAS, G. C., and EARLE, E. D. (1964).—*Nucl. Phys.* **52**: 45.
- THOMPSON, M. N., TAYLOR, J. M., SPICER, B. M., and BAGLIN, J. E. E. (1965).—*Nucl. Phys.* **64**: 486.
- THOMPSON, M. N., TAYLOR, J. M., and WEBB, D. V. (1965).—*Phys. Lett.* **14**: 223.
- ULLRICH, H. (1964).—*Phys. Lett.* **12**: 114.
- VARGA, L. (1961).—*Nucl. Instrum. Meth.* **14**: 24.
- WEISSKOPF, V. F., and EWING, D. H. (1940).—*Phys. Rev.* **57**: 472.
- WHALING, W. (1958).—In "Handbuch der Physik." (Ed. S. Flügge.) Vol. 34. p. 193. (Springer: Berlin.)
- WYCKOFF, J. M., ZIEGLER, B., KOCH, H. W., and UHLIG, R. (1965).—*Phys. Rev.* **137**: B576.
- YERGIN, P. F., AUGUSTSON, R. H., KAUSHAL, N. N., MEDICUS, H. A., MOYER, W. R., and WINHOLD, E. J. (1964).—*Phys. Rev. Lett.* **12**: 733.
- ZIEGLER, B. (1960).—*Nucl. Phys.* **17**: 238.

